

Supporting Information

Glycerol-based Sustainably Sourced Resin for Volumetric Printing

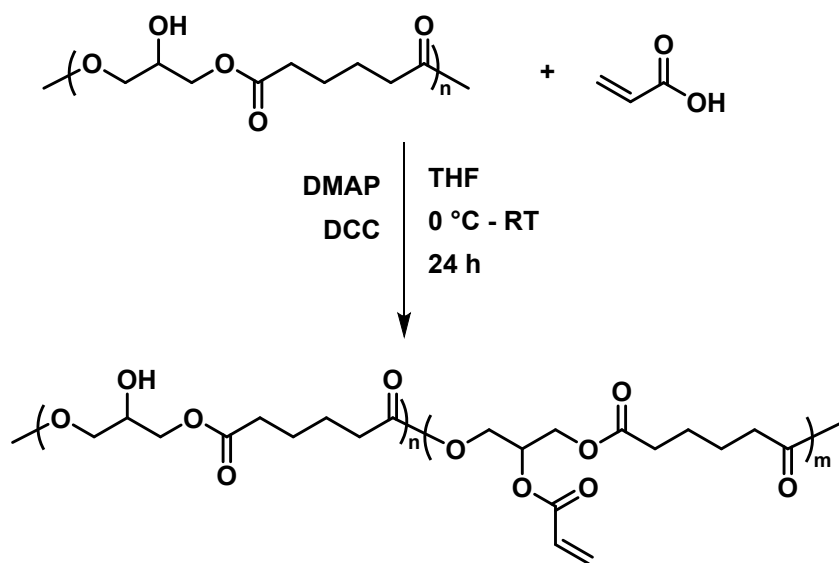
Eduards Krumins,^{a‡} Joachim C. Lentz,^{a‡} Ben Sutcliffe,^b Ali Sohaib,^c Philippa L. Jacob,^a Benedetta Brugnoli,^d Valentina Cuzzucoli Crucitti,^c Robert Cavanagh,^{e,b} Robert Owen,^b Cara Moloney,^e Laura Ruiz-Cantu,^c Iolanda Francolini,^d Steven M Howdle,^a Maxim Shusteff,^f Felicity R. A. J. Rose,^b Ricky D. Wildman,^c Yinfeng He^{c*} and Vincenzo Taresco^{a*}

- a. School of Chemistry, University of Nottingham, Nottingham, NG7 2RD, United Kingdom
- b. School of Pharmacy, Nottingham Biodiscovery Institute, University of Nottingham, NG7 2RD, Nottingham, United Kingdom
- c. Faculty of Engineering, University of Nottingham, Nottingham, NG7 2RD, UK,
- d. Department of Chemistry, Sapienza University of Rome, Piazzale A. Moro 5, 00185 Rome, Italy
- e. School of Medicine, University of Nottingham Biodiscovery Institute, University of Nottingham, NG7 2RD, United Kingdom
- f. Lawrence Livermore National Laboratory, Livermore, CA 94550, USA
- g. Nottingham Ningbo China Beacons of Excellence Research and Innovation Institute, University of Nottingham Ningbo China, Ningbo 315100, China

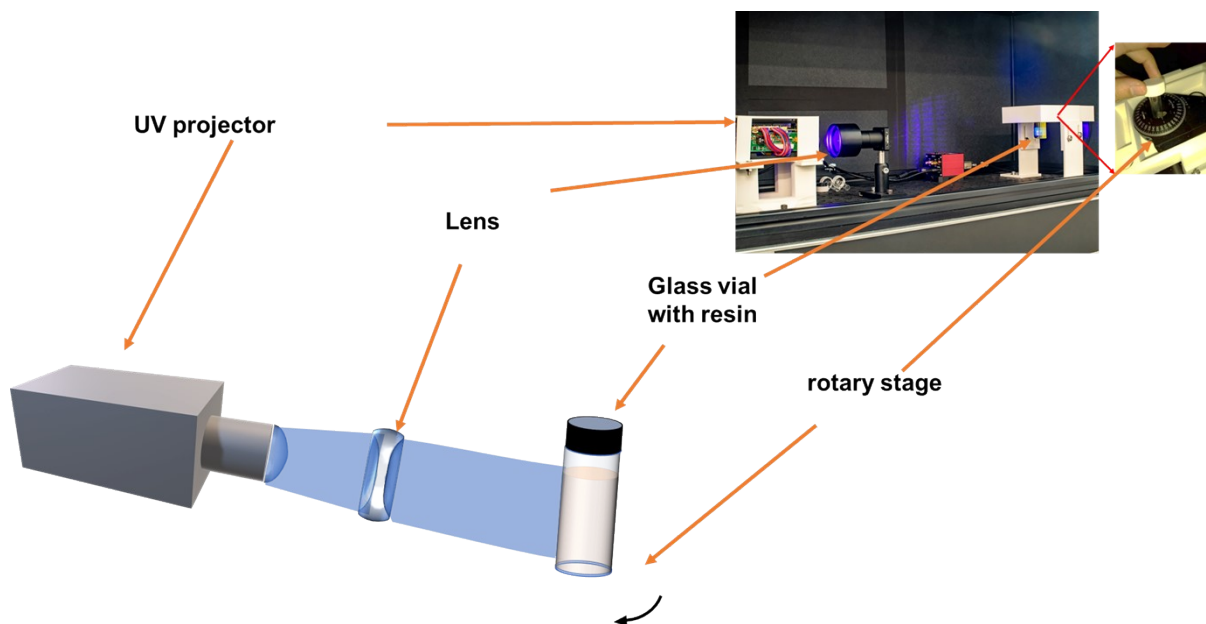
‡ Authors contributed equally.

* Corresponding authors: Yinfeng.He@nottingham.ac.uk,
Vincenzo.Taresco@nottingham.ac.uk

Schemes, Figures and Tables



SI Scheme 1. Synthesis of PGA-A via Steglich esterification.

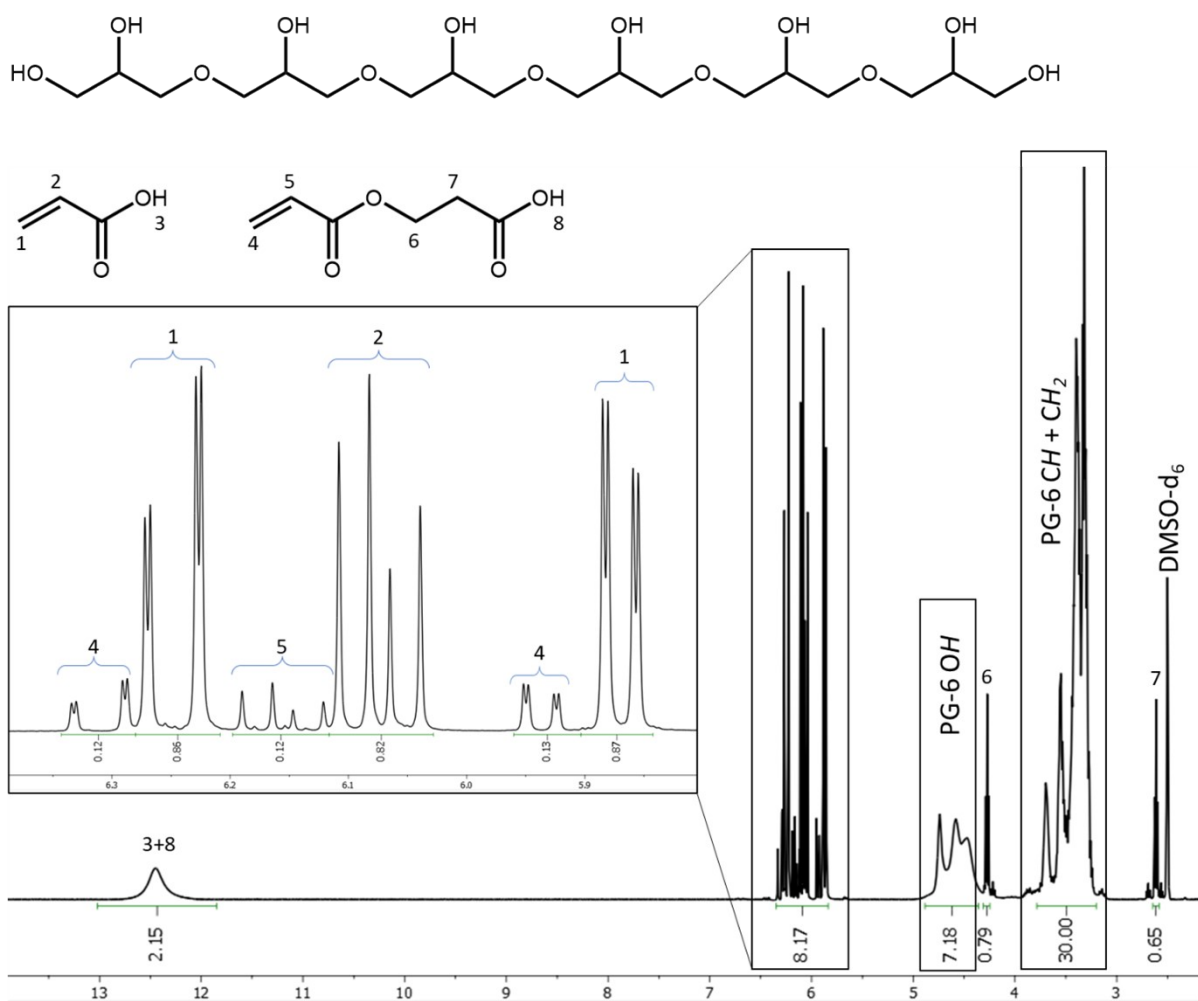


SI Figure 1 Computed Axial Lithography (CAL) setup consisting of a projector, optics, and a rotary stage (based on hardware design files available from <https://github.com/computed-axial-lithography>).

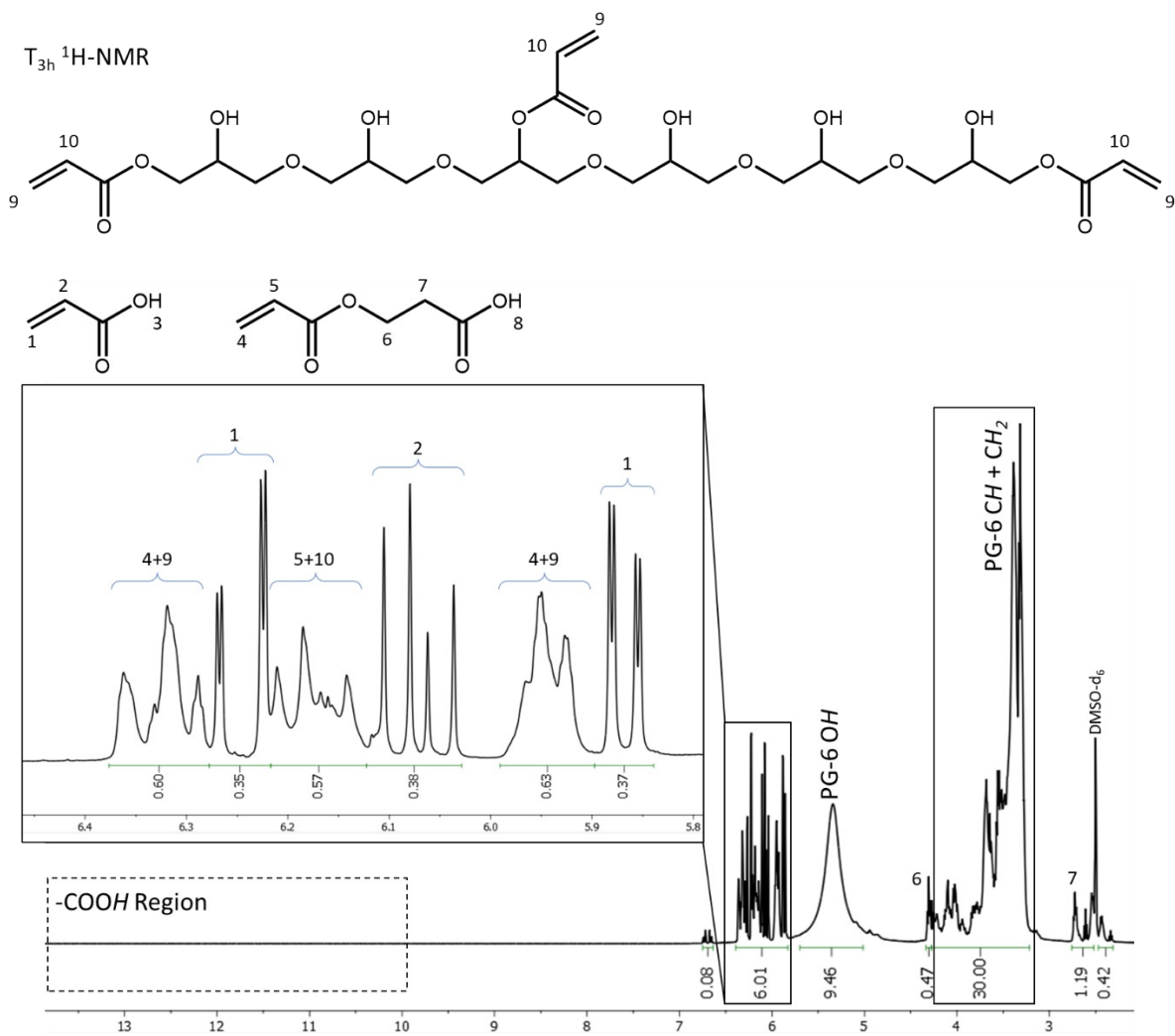


SI Figure 2. *Vial containing PG6-acrylate resin.*

T₀ ¹H-NMR



SI Figure 3. ¹H-NMR at Time Zero of resin synthesis. Note the presence of a -COOH signal around 12.5 ppm, and the presence of Michael addition product in the acrylic acid starting material.



SI Figure 4. 1H -NMR at Time=3 h of resin synthesis. Inset showing the acrylate region of the spectrum. New signals corresponding to acrylate esters have formed. Conversion of acrylic acid is calculated to be approximately 63%, using the integrals of signals assigned 4+9 and 1. Some error in this estimation is a result of signal overlap between acrylic esters with the Michael addition product.

SI Table 1 Acid Values of the reaction mixture with correction applied to account for the presence of catalytic sulphuric acid (AV of batch used= 1112 mg KOH g⁻¹). Conversion was calculated following SI Equation 1.

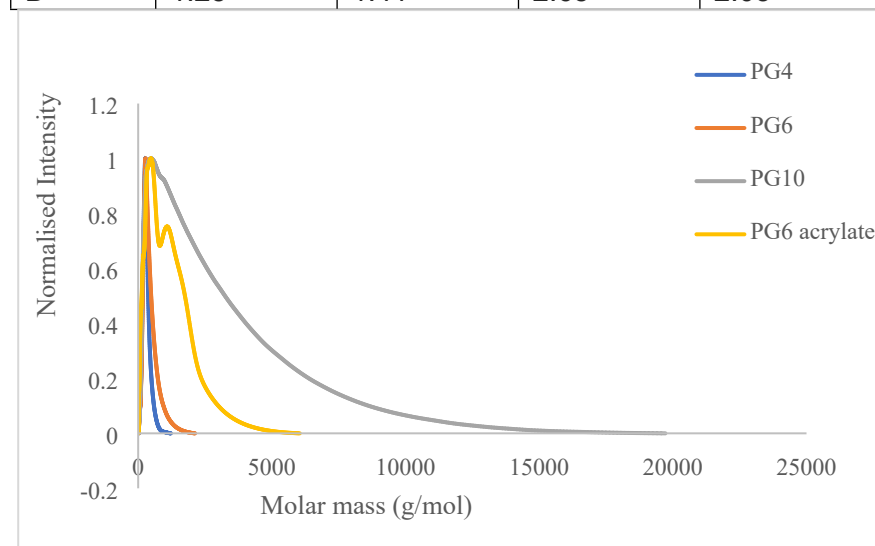
Time (h)	AV (mg KOH g ⁻¹ sample)	Conversion of Acrylic Acid (%)
0	220.4	0
3	55.0	75

$$\text{Conversion (\%)} = 100 \times \left(1 - \frac{\text{AV Time zero}}{\text{AV Time X}}\right)$$

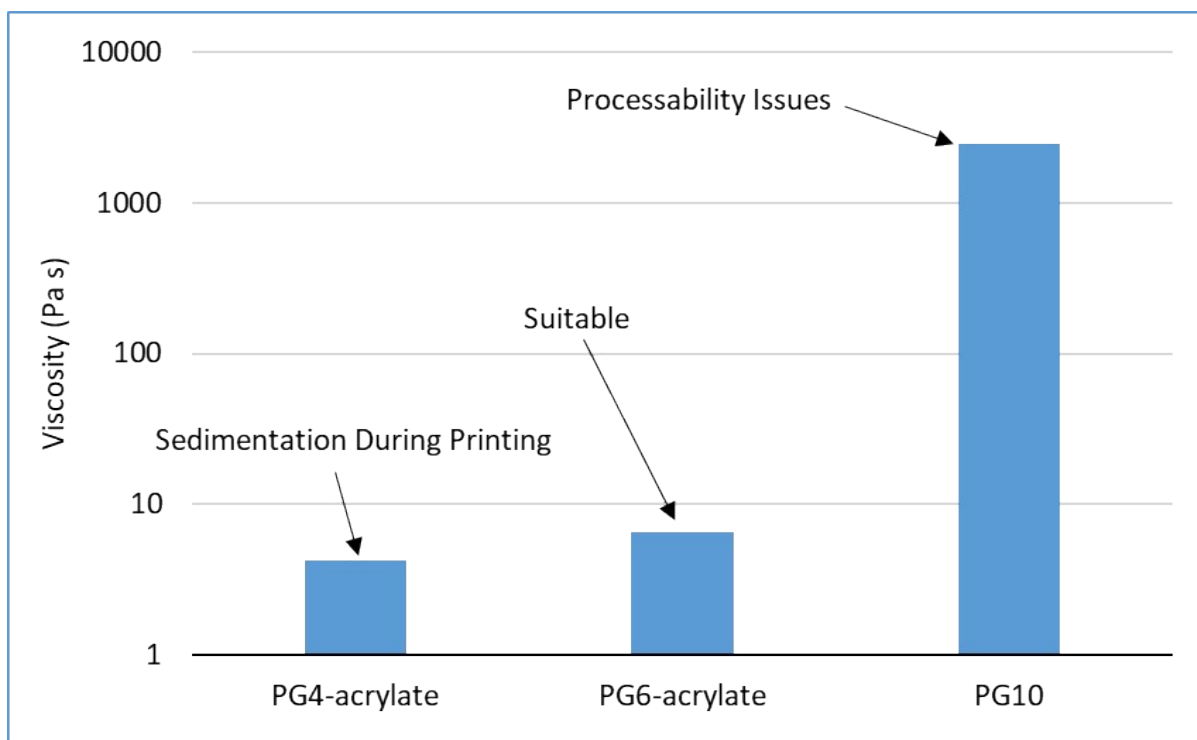
SI Equation 1 Conversion of acrylic acid (%) from acid value obtained at time zero and at measured timepoint during PG6-acrylate synthesis.

SI Table SEC

	PG4	PG6	PG10	PG6 acrylate
M _n	250.0	330.0	1230.5	609.0
M _w	315.0	467.0	3270.0	1233.0
Đ	1.25	1.41	2.65	2.03



SI Table and Figure SEC – Molar masses (g/mol) and Đ for PG4, PG6, PG10, and PG6 acrylate. Measured via aqueous SEC.



SI Figure 5. Viscosity of PG4-acrylate, PG6-acrylate, and PG10 at 25 °C, shear rate of 10 s^{-1} . Due to low viscosity, rapid sedimentation of the cured resin was observed with PG4-acrylate. PG10's viscosity made the resin synthesis impractical. PG6-acrylate's viscosity was found to be in the desired region.

SI Table 2. Volumetric Printing Optimisation of virgin Resin. Print result was assessed visually based on physical appearance of the print on a scale from 1 to 10, where 1 denotes a poor print and 10 an excellent print. Parts marked with an asterisk (*) were produced using two consecutive printing cycles.

Part	Vial size (mL)	Exposure per frame (s)	Frames	Total Exposure Time (s)	Rotation per Frame (°)	Result
cylindrical structures	4	0.1	120	12	3	1
cylindrical structures	4	0.1	40	4	9	2
cylindrical structures	4	0.1	60	6	6	10
Chess piece	4	0.1	60	6	6	10
Ball in cage	20	0.1	60	6	6	1
Ball in cage	20	0.12	60	7.2	6	2
Ball in cage	20	0.12	120	14.4	3	3
Ball in cage	20	0.12	210	25.2	3	4
Ball in cage	20	0.12	160	19.2	3	6
Ball in cage	20	0.12	150	18	3	9
Rectangle	20	0.1	60	6	3	10
Thinker*	20	0.11 + 0.11	120 + 120	26.4	3	9
Rabbit*	20	0.12 + 0.15	120 + 30	18.9	3	9
Tensile bar	20	0.12	60	7.2	6	6
Tensile bar	20	0.12	120	14.4	3	9

SI Table 3. Volumetric Printing Optimisation of Recycled Resin. Print result was assessed visually based on physical appearance of the print on a scale from 1 to 10, where 1 denotes a poor print and 10 an excellent print.

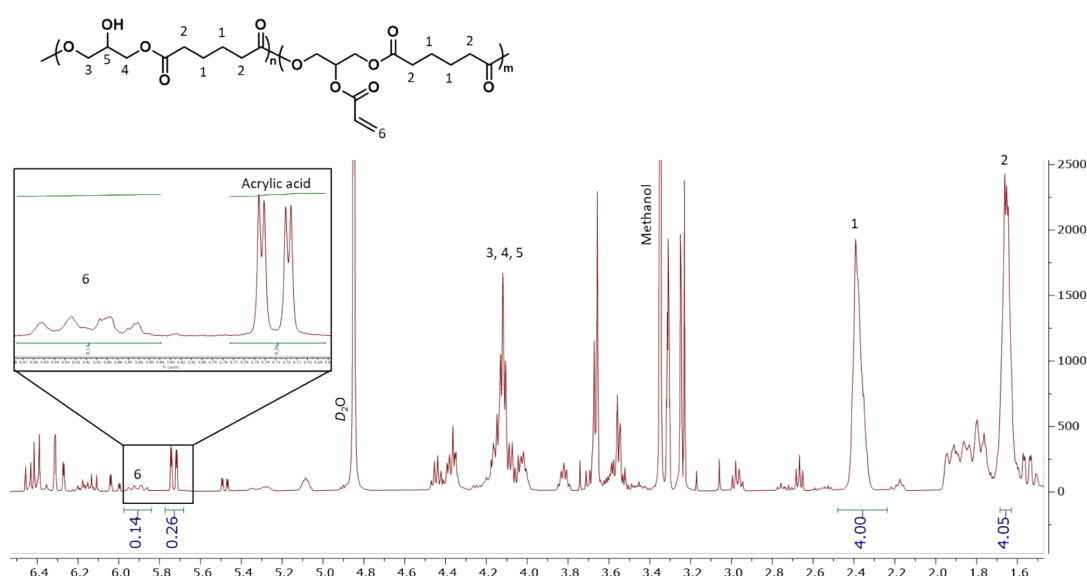
Part	Vial size (mL)	Exposure per frame (s)	Frames	Total Exposure Time (s)	Rotation per Frame (°)	Result
cylindrical structures	20	0.12	120	14.4	3	10
cylindrical structures	20	0.12	140	16.8	3	7
cylindrical structures	20	0.12	120	12	3	10

SI Table 4. Volumetric Printing Optimisation of PGA-AA Doped Resin. Print result was assessed visually based on physical appearance of the print on a scale from 1 to 10, where 1 denotes a poor print and 10 an excellent print.

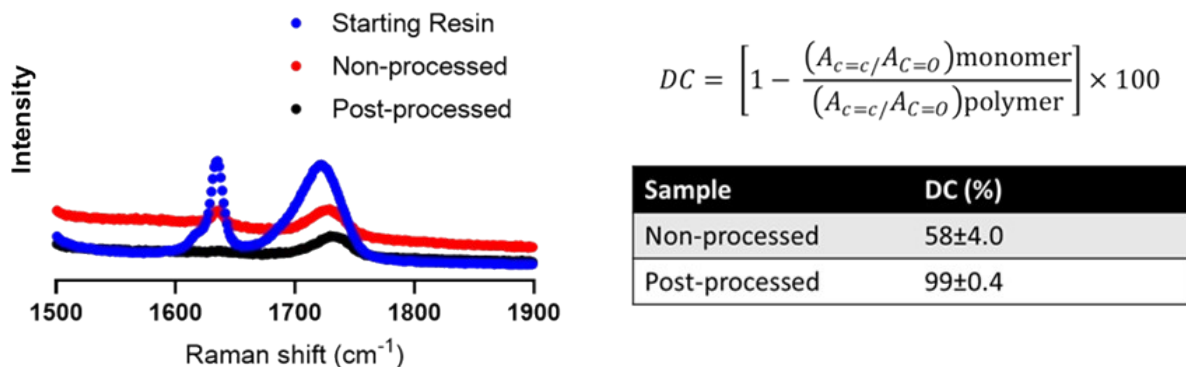
Part	PGA Content (wt.%)	Vial size (mL)	Exposure per frame (s)	Frames	Total Exposure Time (sec)	Rotation per Frame (°)	Result
cylindrical structures	5	20	0.1	120	12	3	8
cylindrical structures	10	20	0.125	120	15	3	7
cylindrical structures	20	20	0.1	100	10	3	10

SI Table 5. Volumetric Printing Optimisation of 10,12-Pentacosadynoic Acid (PCDA) Doped Resin. Print result was assessed visually based on physical appearance of the print on a scale from 1 to 10, where 1 denotes a poor print and 10 an excellent print.

Part	PCDA Content (wt.%)	Vial size (mL)	Exposure per frame (s)	Frames	Total Exposure Time (s)	Rotation per Frame (°)	Result
cylindrical structures	10	4	0.12	60	7.2	6	5
cylindrical structures	10	4	0.12	80	9.6	3	5
cylindrical structures	10	4	0.12	40	4.8	6	8
cylindrical structures	20	4	0.12	40	4.8	6	8
cylindrical structures	30	4	0.12	40	4.8	6	3



SI Figure 6. ¹H-NMR spectrum of PGA-A in D₂O demonstrating ~14% functionalisation of pendant OH bonds along polymer backbone of PGA.



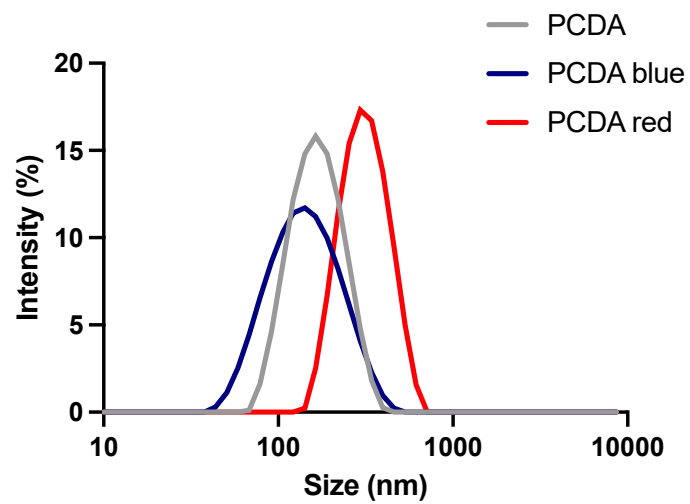
SI Figure 7. Raman Spectroscopy to assess degree of curing (DC). Left, Stacked Raman spectra of an example of starting resin, printed resin (non-processed) and resin post curing (post-processed) in the Raman shift range between 1500-1900 cm^{-1} . Right, DC was determined by measuring the change in the ratio of peak areas associated with the C=C ($\approx 1634 \text{ cm}^{-1}$) and C=O ($\approx 1720 \text{ cm}^{-1}$) bonds before and after polymerisation.

SI Table 6. Storage modulus of printed cylindrical samples with increasing PGA-A loading.

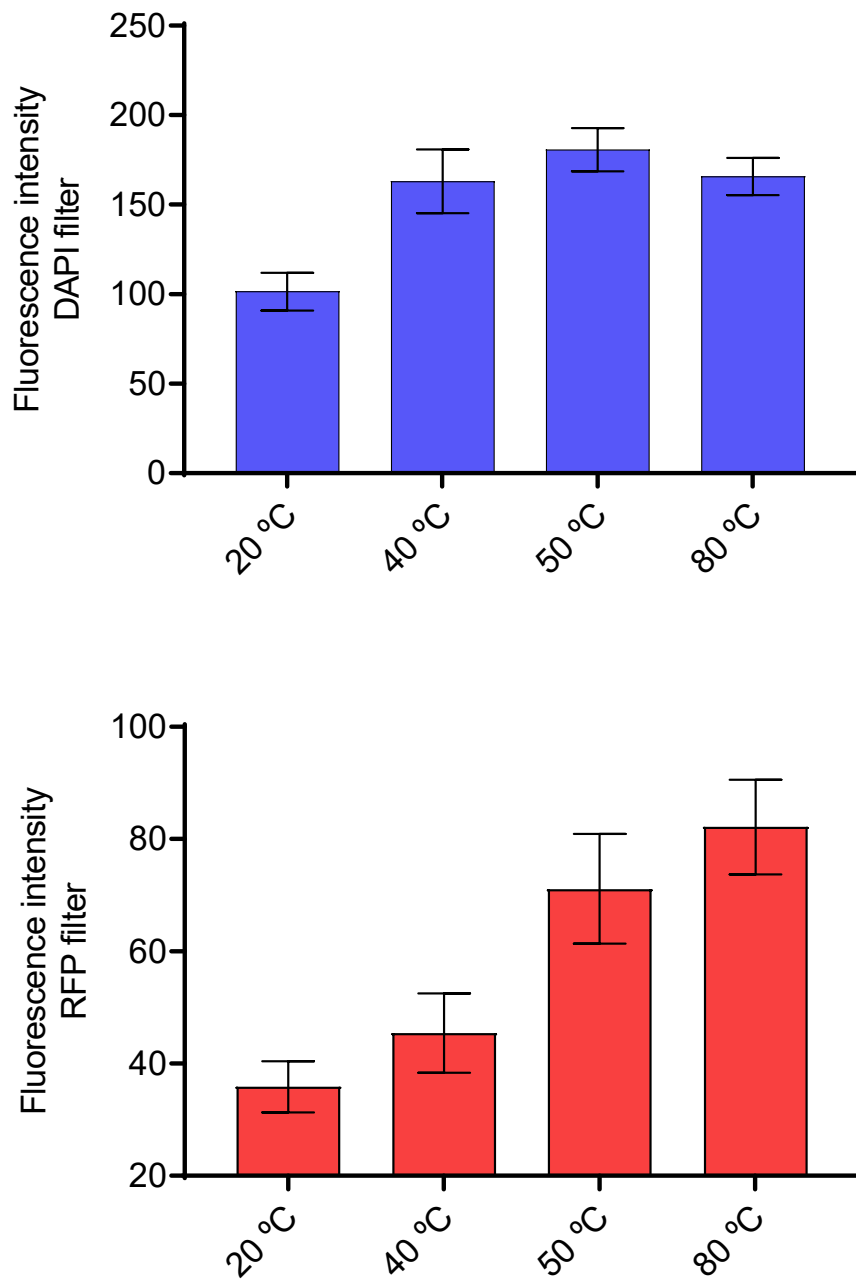
PGA-A Loading (wt%)	Storage Modulus (kPa)
0	2221
5	450
20	522

SI Table 7. Size of PCDA nanosystems non-polymerised, polymerised (blue) and after thermal stimulus (red)

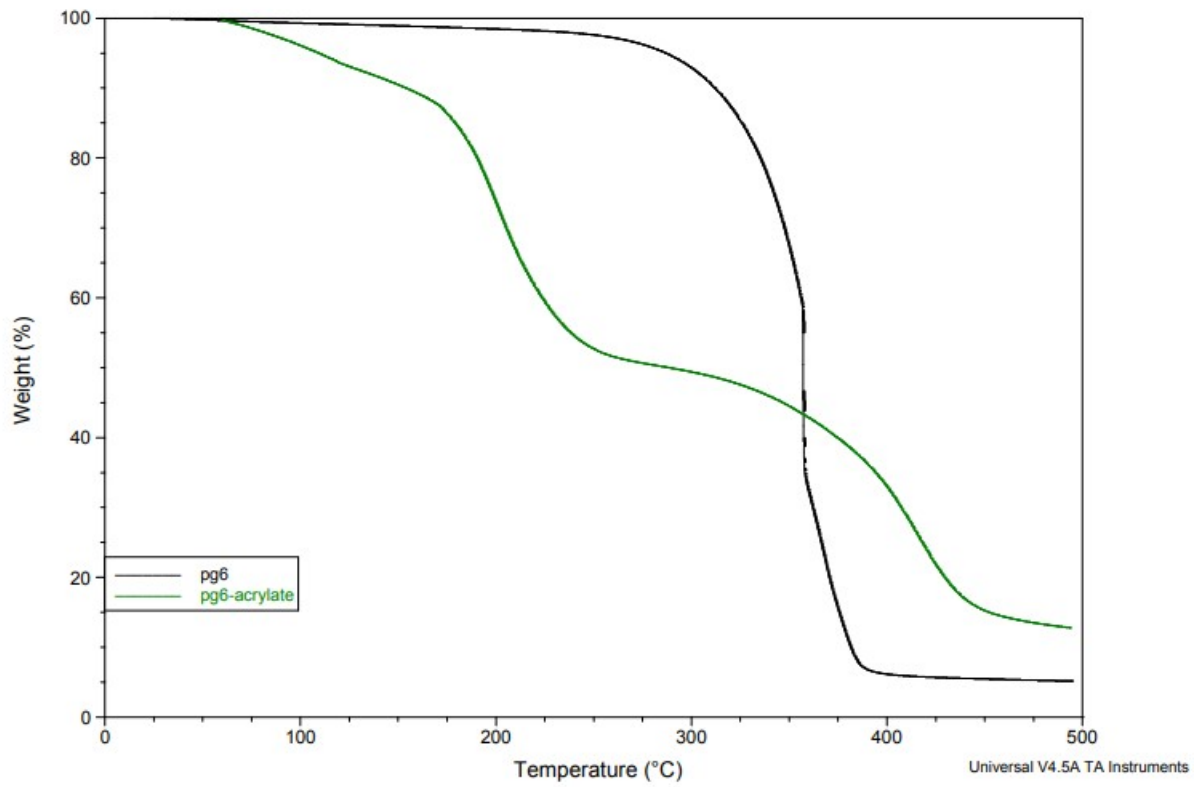
Sample	Hydrodynamic diameter (nm)	PDI
PCDA	152.1 ± 0.1	0.12 ± 0.10
PCDA blue	120.3 ± 0.5	0.21 ± 0.01
PCDA red	293.2 ± 0.8	0.10 ± 0.01



SI Figure 8. DLS traces of PCDA nanosystems non-polymerised (grey), polymerised (blue) and after thermal stimulus (red).



SI Figure 9. Fluorescence Intensities during microscopy, blue (top) and red (bottom) of the samples seen in Figure 4 of the main text. Data presented as mean \pm S.D; $n=3$.



SI Figure TGA. TGA of PG6 and PG6 acrylate